



Residual stress stability of HFMI-treated transverse attachments under variable amplitude loading with the P(1/3) and the linear spectrum

Daniel Löschner¹ · Paul Diekhoff² · Richard Schiller¹ · Imke Engelhardt¹ · Thomas Nitschke-Pagel² · Klaus Dilger²

Received: 4 October 2022 / Accepted: 24 January 2023 / Published online: 2 February 2023
© The Author(s) 2023

Abstract

The potential of HFMI treatment to increase fatigue life under service loading remains in debate. However, some recent studies show that even under variable amplitude loading (VAL), fatigue strength is increased compared to untreated welds. Discussions generally focus on the stability of initial compressive residual stresses, which may be reduced during VAL due to high peak stresses. In this context, the potential of HFMI treatment is often only attributed to residual stress stability. This study presents further results on the effect of VAL with a P(1/3) and a linear load spectrum on the residual stress stability of HFMI-treated transverse stiffeners (TS) made of mild steel (S355) and high-strength steel (S700M). The impact of random, High-Low and Low-High loading sequences on the fatigue strength as well as on the residual stress behaviour of HFMI-treated joints will be discussed.

Keywords Fatigue of welded joints · High Frequency Mechanical Impact (HFMI) – treatment · Constant and Variable amplitude loading · Random · High-Low · Low-High · Linear spectrum · P(1/3) spectrum · Transverse attachments · Sequence effect · Residual stresses stability

Nomenclature

AW as welded
CAL constant amplitude loading

f_y nominal yield strength
 H_0 spectrum length
HFMI high-frequency mechanical impact treatment
HL high-Low loading sequence
I irregularity factor
LH low-high loading sequence
LS longitudinal stiffener
MPa megapascal
 P_s survival probability
R stress ratio
random randomly distributed loading sequence
TS transverse stiffeners
VAL variable amplitude loading
 $\Delta\sigma_{50\%}$ fatigue strength at $2 \cdot 10^6$ cycles with $P_s = 50\%$
 $\sigma_{a,max}$ maximum applied stress amplitude during VAL
 $\sigma_{RS,ini}$ maximum initial residual stress level
 $\sigma_{RS,sp}$ residual stress reduction after first spectrum pass
 σ_{RS}^T transverse residual stresses
 $M_{0,1,\dots,i}$ measuring points, on which fatigue tests were interrupted for the continuous residual stress analysis

Recommended for publication by Commission XIII - Fatigue of Welded Components and Structure

✉ Daniel Löschner
loeschner.daniel@hm.edu
Paul Diekhoff
p.diekhoff@tu-braunschweig.de
Richard Schiller
richard.schiller@hm.edu
Imke Engelhardt
imke.engelhardt@hm.edu
Thomas Nitschke-Pagel
t.pagel@tu-braunschweig.de
Klaus Dilger
k.dilger@tu-braunschweig.de

¹ Laboratory for Steel and Lightweight Structures, Institute for Material and Building Research, University of Applied Science Munich, Munich, Germany

² Institute of Joining and Welding, Technische Universität Braunschweig, Braunschweig, Germany

1 Introduction

The strength-increasing and thus fatigue life-extending impact of High-frequency mechanical impact (HFMI)-treatment is based on an improvement of the weld toe geometry, a local surface hardening and the induction of compressive residual stresses. The potential for fatigue life improvement of welds by HFMI-treatment has already been confirmed for various welded details made of different steel grades in numerous studies. Guidelines published in 2016 [1] and 2019 [2] summarise the results of these studies and assess the fatigue strength improvement depending on the steel grade, welded detail and stress ratio. As mentioned in [3, 4] these guidelines are mostly based on the results of fatigue tests under constant amplitude loading (CAL). Further research focuses on the influence of near-service VAL with different spectra on the fatigue performance of HFMI-treated welds [4–10].

Yildirim et al. examined in their study [8] the fatigue behaviour of HFMI-treated longitudinal stiffeners (LS) made of S700 under VAL. Fatigue test results under fully reversed ($R = -1$), randomly distributed VAL with a straight-line spectrum, show that the beneficial compressive residual stresses induced by HFMI are significantly reduced during service loading. Although the fatigue strength was increased by HFMI treatment, the degree of improvement is significantly lower compared to CAL. This outcome is in line with the results of Leitner et al. [9] and Marquis [11]. Fatigue tests in [9] incorporate LS of S355 and S700 at a stress ratio of $R = 0.1$ and $R = -1$ applying a straight-line distribution. Marquis [11] performed fully reversed ($R = -1$) VA fatigue tests on LS made of steels S700 and S960 utilizing a straight-line spectrum as well. In [4, 5], studies focus on the sequence effect of VAL ($R = -1$) with different spectrum shapes on the fatigue behaviour of transverse stiffeners (TS) made of S355 and S700. The results of these studies reveal that under VAL the fatigue strength improvement due to HFMI treatment is comparable to CAL.

When comparing these studies, no overall conclusive statement can be provided on the fatigue behaviour of HFMI-treated welds under VAL. While the studies in [8, 9, 11] on LS show that fatigue strength increase relative to the as-welded (AW) state is reduced by VAL, studies in [4, 5] on TS prove the enormous potential of this treatment method. It is evident that the fatigue strength improvement under VAL is predominantly affected by the notch effect of the welded detail, the quality of the HFMI-treatment, the steel grade and the service loading characteristics, such as spectrum shape, stress ratio and peak stresses. It is therefore not surprising that the effectiveness of HFMI treatment under VAL remains highly debated.

Deviations occur for the damage accumulation calculation as well. Based on the evaluation of fatigue tests on TS of different steel grades (S355, S690, S960) with a stress ratio of $R=0.1$ under blocked VAL real damage sums of $D_{\text{real}} = 0.5$ for high strength steels to $D_{\text{real}} = 1$ for mild steels are evaluated, taking into account the experimentally derived SN curves [7]. The analysis of the results from the experiments in [4, 5] shows that, based on the experimental SN curves, a damage sum of $D_{\text{real}} < 0.5$ is calculated for specimens made of both S355 as well as S700. These deviations in the calculations of real damage sums indicate the sensitivity in the assessment of HFMI-treated welds under VAL applying a linear damage accumulation method. In continuation of the work already mentioned [8, 9], a subsequent study [10] focuses on the fatigue assessment of HFMI-treated steel joints under VAL respecting the FAT class for HFMI in [1]. It was concluded that applying the recommended value of the specified damage sum of $D = 0.5$ leads to a conservative fatigue assessment in all cases relied to. Even increasing the value to $D = 1.0$ still leads to a conservative assessment. As mentioned before, the efficiency of such treatments within the scope of the guideline [1] is mainly attributed to the compressive residual stresses induced. It is often argued that due to service loading, e.g. under VAL, especially due to high peak stresses, the initial residual stresses may be reduced when the local yield strength is exceeded. Consequently, it is assumed that the initial benefit of such a treatment method is reduced or completely dissolved with the relaxation of compressive residual stresses [8]. For this reason, the increase of FAT-classes in [1, 2] is related to the applied stress ratio and the allowable peak stresses of the service loading are limited according to the material's yield strength.

Mikkola et al. [12] have shown that compressive peak stresses of $0.6 \cdot f_y$ (nominal yield strength) resulted in full residual stress relaxation on treated LS. However, they observed, that fatigue improvement could be expected even after significant residual stress relaxation. Leitner et al. [13] observed that the residual stresses of TS are already significantly reduced during the first load-cycles. Results are in common with the study on butt welds in [14].

However, the beneficial effect of the strain-hardened surface layer due to the HFMI treatment is not necessarily affected [15]. Preliminary investigations on TS in [4, 5] shows that even at high peak stresses of VAL, the fatigue life remains increased by HFMI compared to the as welded state. Even a significant impact of the loading sequence between High-Low- and Low-High ordered block loading on the service life could not be observed on HFMI-treated specimens. Assuming that the fatigue behaviour is mainly influenced by the initial residual stresses, the following may be concluded. Either the residual stresses are stable when subjected to VAL

or, if relaxation is occurring, the fatigue performance may not be mainly affected by the residual stress state.

Therefore, it is interesting when and how residual stresses may be reduced when subjected to service loads. In addition, it is appropriate to question which benefit regardless of the initial residual stresses, may extend the fatigue life. This study focuses on the effect of VAL on the initial residual state. Therefore, uniaxial fatigue tests with constant and variable amplitude loading on transverse attachments were performed. Results were published in [4, 5]. Along with the previous work, the effect of VAL on the stability of the residual stresses and the influence of the loading sequence on the relaxation behaviour is shown in this paper. Furthermore, the correlation between the fatigue improvement and the residual stress stability will be discussed.

2 Experimental work

2.1 Load sequences, specimen, and testing procedure

The impact of service loads on the residual stress stability HFMI-treated joints was studied by performing uniaxial fatigue tests with constant and variable amplitude loading on TS. The VAL tests were performed with different load sequences — random (R), High-low (HL) and Low-high (LH) — of a P(1/3) and linear shaped spectrum. The different sequences as well as the spectrum shapes are qualitatively

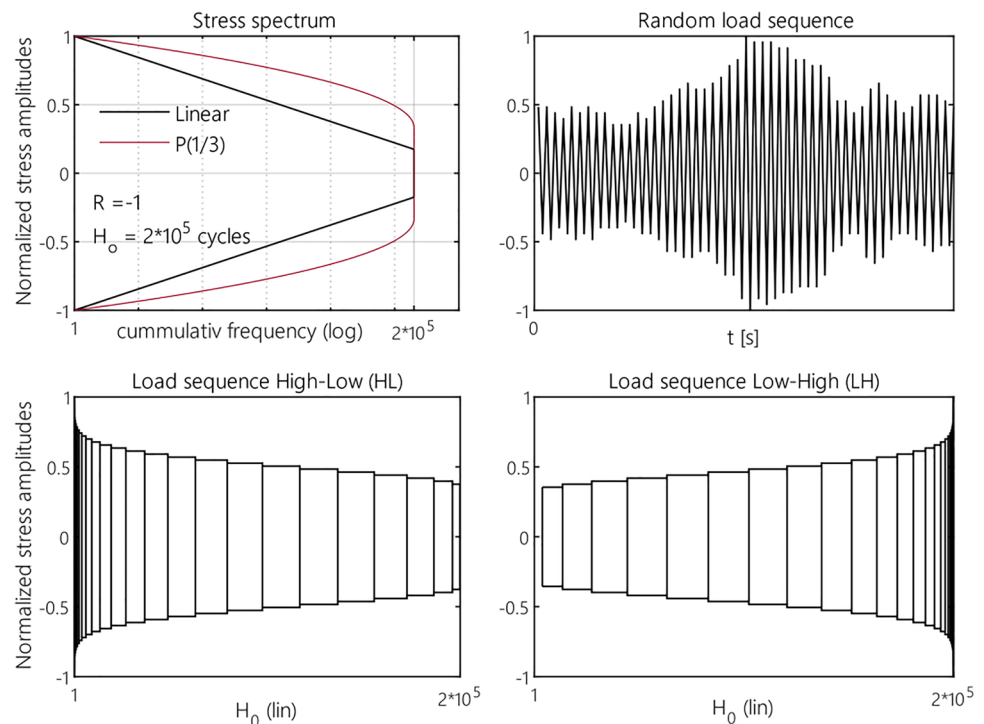
explained in Fig. 1. The spectrum length of the random load sequence is set to $H_0 = 200,000$ load-cycles with an irregularity factor of $I = 0.99$ and a stress ratio of $R = -1$. The generation of the random and blocked (HL, LH) loading sequences is based on the approach outlined in [4, 5].

The different load sequences are supposed to provide information about when and how residual stresses relax during the VAL and how the relaxation behaviour affects the corresponding fatigue behaviour. The stress ratio of $R = -1$ is set to reduce the impact of fluctuating mean stresses on the test results and on damage accumulation. In addition, the use of a stress ratio of $R = -1$ enables the effects of compressive and tensile peak stresses on fatigue behaviour of HFMI treated welds to be examined. Furthermore, the influence of tensile and compressive peak stresses during service loading up to $0.9 \cdot f_y$ on residual stress relaxation is studied in scope of this work.

A transverse attachment was chosen as the weld detail to be investigated due to extensive test results under CAL and the relative high notch effect. The design and dimensions of the specimens are shown in Fig. 2 and have been chosen according to [17] so that cracking from the rounding should be avoided. The joints were fabricated out of mild (S355J2+N) and high strength steel (S700M). The chemical composition and the corresponding material properties as well as the welding process and HFMI-treatment parameters are outlined in [4, 5, 16].

The fatigue tests were performed under alternating uniaxial load at the Institute of Joining and Welding of the

Fig. 1 Studied sequences and stress spectrum [16]



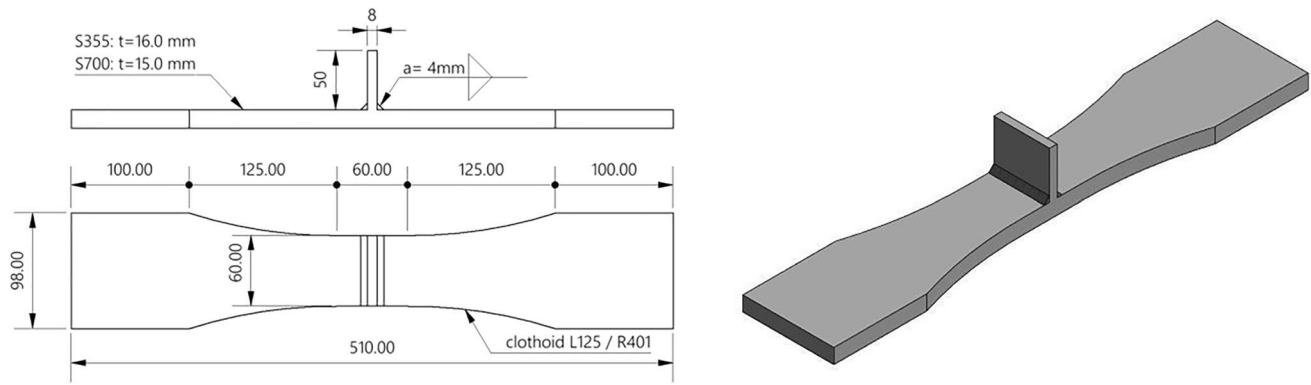


Fig. 2 T-joint specimen dimensions [16]

Table 1 Parameters of the X-ray residual stress measurement

Parameter	Value
Radiation	Cr-K α
Diffraction line	Fe α {211}
2 Θ	156°
Collimator size	2 mm
Counting time	60 s
DEK	$s_1 = -1.27 \times 10^{-6} \text{ MPa}^{-1}$ and $\frac{1}{2} s_2 = 5.8 \times 10^{-6} \text{ MPa}^{-1}$

University of Braunschweig and at the Laboratory for Steel and Lightweight Structures of the Munich University of Applied Sciences. While CAL fatigue tests were conducted on servo-hydraulic and resonance testing machines, VAL tests were carried out entirely on servo-hydraulic machines. X-ray diffraction measurements and macro-hardness analyses were performed. To evaluate the residual stress stability under different loading conditions and to determine the influence of service loading and loading sequence on the condition of the HFMI-treated boundary layer, surface residual stress profiles were recorded by X-ray diffraction measurements.

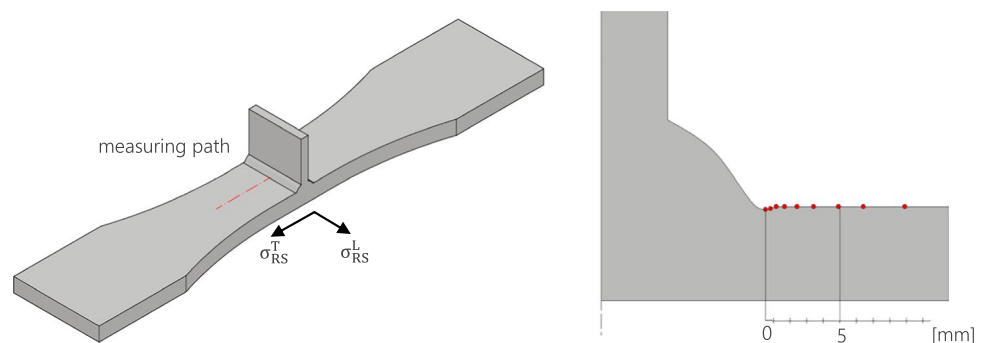
3 Investigation on residual stress stability

3.1 Procedure

The surface residual stresses of the welded specimens were determined by X-ray diffraction. Important measurement and evaluation parameters can be found in Table 1. The longitudinal (welding direction) and transverse residual stresses (loading direction) were measured. The evaluation was performed using the $\sin^2\psi$ method.

The residual stresses were measured on different specimens to determine the influence of the material and the treatment process. The measurements were obtained in the centre of the specimen from the weld toe to the base material. As no significant differences in the residual stress profiles of both sides have been expected due to the symmetry, the measurement results of one side are presented in the following. Figure 3 illustrates the measuring path on the specimens with the individual measuring points. The first point per measurement sequence is located directly at the weld toe in the AW state and the middle of the treated zone for HFMI-treated specimens. The increment between the two consecutive points was enlarged with increasing distance to the weld toe from 0.5 to 5 mm.

Fig. 3 Measuring points at the weld toe of the specimens



First, the residual stress states of transverse stiffeners in the AW state and the HFMI-treated state are compared. Subsequently, the investigations regarding the residual stress stability under quasi-static, cyclic CAL and VAL of different spectrum shapes are presented. Table 2 shows the experimental matrix of the residual stress measurement conducted.

A more detailed evaluation regarding the effects of the HFMI treatment on the surface layer depth profiles of the initial residual stress state was recorded for both materials to analyse the depth impact of the HiFIT or PITec treatment. For this purpose, X-ray residual stress measurements were carried out on the surface layer after stepwise electrolytic abrasion to a depth of about 0.5 mm.

For the evaluation of residual stress stability, many different measurements were conducted. The studies are divided into measurements after quasi-static and cyclic loading. The change of the residual stress profiles according to different loads were measured exclusively for specimens in the HFMI-treated state.

Since the residual stress state in loading direction is of primary interest only the transverse residual stress profiles are shown in the following chapter. Figure 4 shows an overview of the different loading scenarios applied to the specimens to analyse the residual stress stability.

Residual stress stability after quasi-static loading is analysed by stepwise increasing the load by about 20% of the yield strength and recording the residual stress profiles after each load step. The studies on residual stress stability due to VAL are divided into three categories. In addition to random loading, the collectives of the two spectrum shapes were tested in descending (HL) and ascending (LH) order. Tests were carried out for each spectrum (P1/3 and linear) and each material (S355J2+N and S700M). The spectrum length of each shape was set to about 200,000 cycles. During the

fatigue test with random VAL, the residual stresses were measured at the end of a fully passed spectrum. For sorted (HL, LH) VAL tests, measurements were taken at four points to check the effect of individual stress levels on the residual stress profile. For this purpose, the sorted VAL tests were interrupted several times to repeatedly measure the residual stress distribution. Interruptions were made after passing through all amplitudes equivalent to 95, 80 and 60% of the maximum spectrum amplitude. Figure 5 shows the spots of the sorted VAL sequences where the tests were interrupted for the measurements (M1–4).

3.2 Results and effect of different loading scenarios on the residual stress state

This chapter first compares the residual stress state of transverse stiffeners in the AW state and HFMI-treated state. Following, the studies regarding the effect of quasi static load on the residual stress relaxation of HFMI-treated weld toes are presented. In the end results of measurements describing the influence of cyclic CAL and VAL on the residual stress distribution of HFMI-treated transverse attachments is shown.

3.2.1 Initial residual stress state

To prepare the specimens for the fatigue tests, the HFMI-treatment methods were assigned to the two different materials. Specimens made of S355J2+N were treated exclusively with the HiFIT device. The PITec device was used for treatment of the S700M-welds Fig. 6 compares the transverse residual stresses at the weld toe area of the specimens made of S355J2+N and S700M before and after HFMI-treatment. The residual stress state is measured on one side of the transverse stiffener in the centre of the specimen from the weld toe to 25 mm into the base metal. The area plastically deformed by HFMI-treatment at the weld toe is highlighted in grey.

For specimens made of S355J2+N, the HFMI treatment induces transverse residual compressive stresses of -100 MPa in the centre of the treated zone. This value increases to about -350 MPa at the edge of the treated zone and decreases subsequently to the initial residual stress level to about -200 MPa at the base material. Measurements on specimens of S700M also show a comparable result. In the transverse direction, residual compressive stresses of -200 MPa appear at the centre of the treated zone. The maximum residual compressive stress of -450 MPa is located outside the transition area at 1.5 mm from the centre of treatment.

Figure 7 shows the transverse residual stress depth profiles in the centre of the HFMI-treated weld toe of S355J2+N and S700M. Whereas for specimen of S355 the transverse residual stresses (σ_{RS}^T) increase from -180 to -230 MPa and then

Table 2 Experimental matrix of the residual stress measurements

Loading/state	S355J2+N		S700M	
	AW	HFMI (HiFIT)	AW	HFMI (PITec)
Initial/surface	X	X	X	X
Initial/depth		X		X
Quasi-static		X		X
CAL		X		X
VAL				
Spectrum	sequence			
P(1/3)	Random	X		X
	High-Low	X		X
	Low-High	X		X
Linear	Random	X		X
	High-Low	X		X
	Low-High	X		X

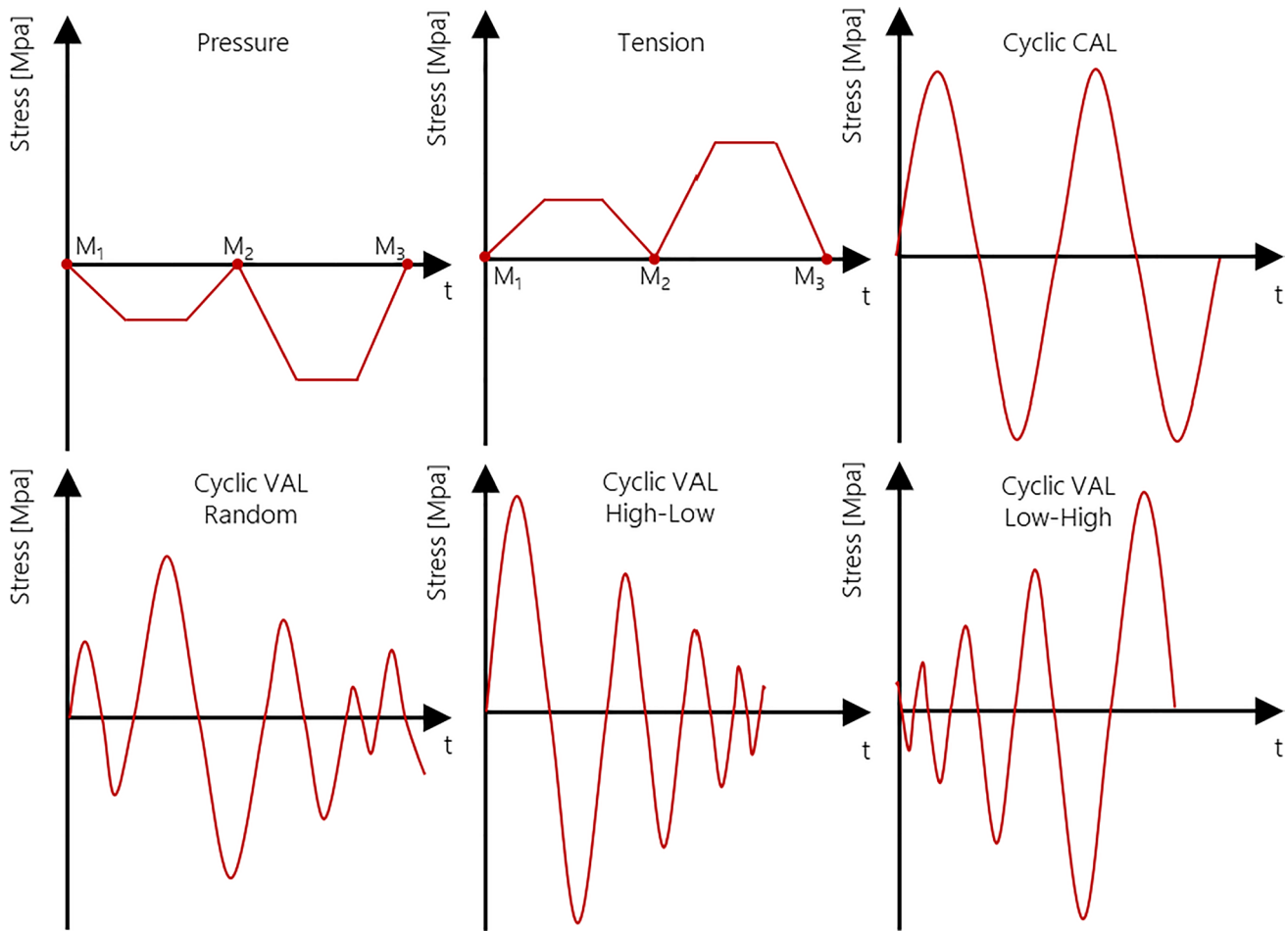
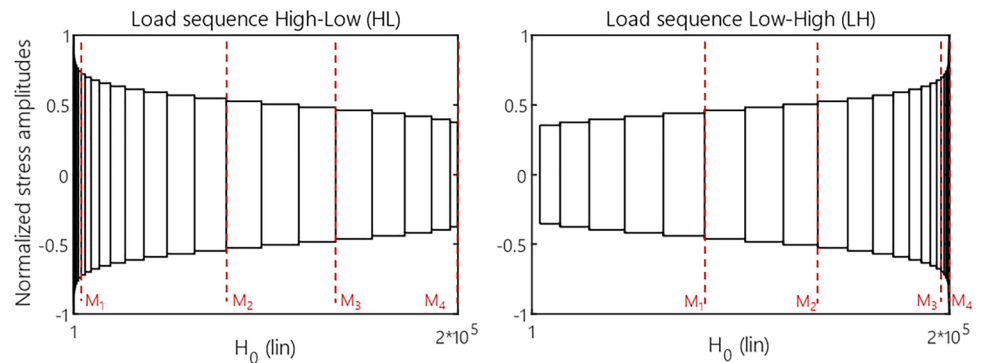


Fig. 4 Simplified load-time histories of the different loading types

Fig. 5 Representation of the spectrum interruption for the continuous residual stress analysis of High-Low (left) or Low-High VAL tests (right)



decrease consistently to -100 MPa, for specimen of S700M the reduction of σ_{RS}^T from -300 to -200 MPa at a depth of 0.5 mm is noticeable consistently.

3.2.2 Quasi-static loading

Figure 8 shows the transverse residual stress profiles after quasi-static tensile (left) and compressive loading (right) of

HFMI-treated weld toes of the steel grade S355. In the initial state, compressive residual stresses in the middle of the treatment are approx. -100 MPa. To investigate the residual stress stability due to quasi-static loading, the load is progressively increased by about 20% of the yield strength and the residual stresses are measured after each load step. No change in the residual stress state is visible up to a load level of about 80 % of f_y .

Fig. 6 Initial residual stress state before and after HFMI-treatment, S355 (left) and S700M (right)

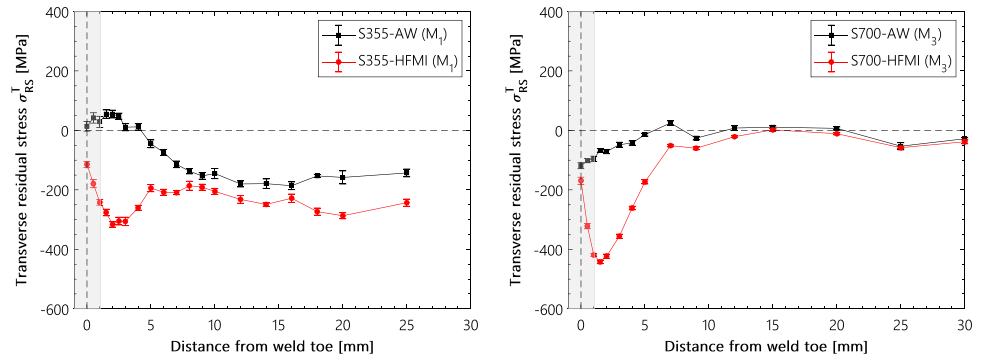


Fig. 7 Initial residual stress depth profiles after HFMI-treatment, S355 (left) and S700M (right)

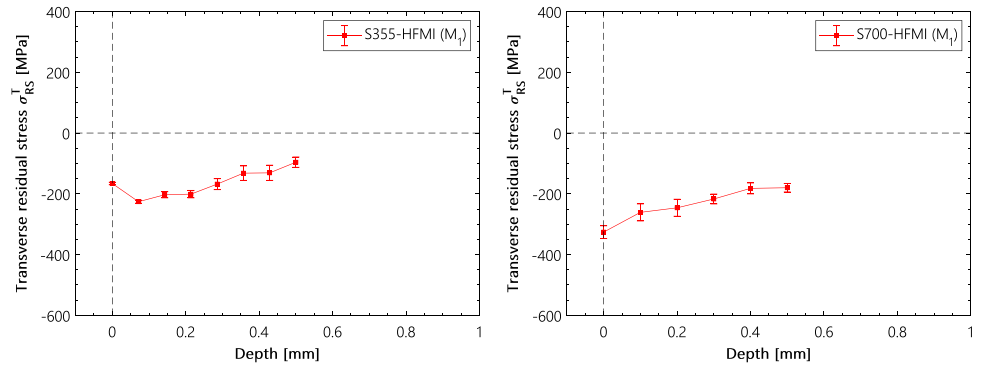


Fig. 8 Transverse residual stress profiles of HFMI-treated transverse stiffeners made of S355 after quasi-static tensile (left) and compressive loading (right)

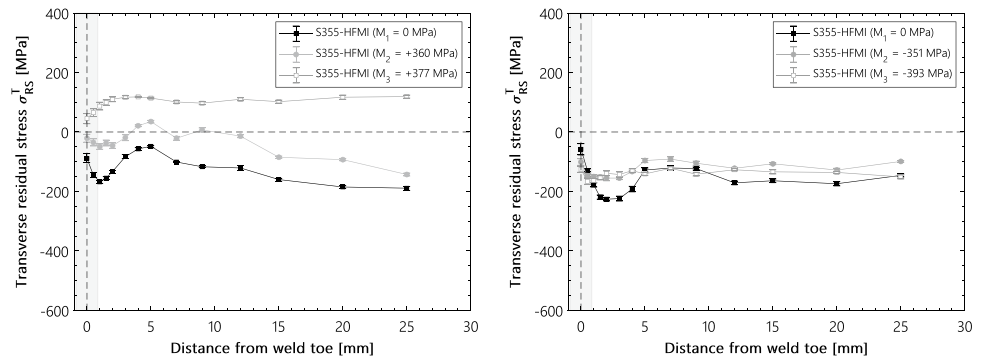


Figure 9 illustrates the effect of quasi-static loads on the residual stress state of transverse stiffeners made of S700M. The high-strength S700M shows a more differentiated response. Due to quasi-static tensile loading, there is a sequential reduction of the maximum residual compressive stresses in the transition area of the HFMI-treated zone from -400 to -300 MPa. In the centre of the treated area, the initial residual stresses are slightly compressive or even tensile. The residual stresses in this zone are initially almost completely relieved from $+125$ to -150 MPa by quasi-static loading. In the case of compressive stress, a significant change in the residual stress can only be observed at a stress level of -550 MPa, whereas the

residual stress relaxation due to tensile loading becomes evident above a level of $+690$ MPa.

3.2.3 Cyclic constant amplitude loading

Figure 10 shows the residual stress profiles near the weld toe after different load cycles due to CAL at a stress ratio of $R = -1$. The plots show the residual stress profiles after 1, 1000 and 100,000 load cycles. The number of cycles for the measurements were chosen to investigate a change of residual stresses with increasing number of cycles, as observed in [13, 18] even for comparatively low stress levels. The stress amplitudes were set to 189 MPa (S355) and to 250 MPa

(S700M). Neither the specimen made of S355 nor the specimen of S700M show a significant change in residual stress state due to CAL. According to the results obtained from quasi-static loading, the change in residual stress due to CAL appears predictable. Due to the low stress amplitude in relation to the material yield strength, a relaxation of residual stress is not observed. The duration and frequency of CAL with increasing number of cycles has no apparent impact on the residual stress profile.

3.2.4 Cyclic variable amplitude loading

High-Low and Low-High blocked loading Figures 11 and 12 compare the residual stress distribution based on different

loading sequences of P(1/3) and linear shaped spectrum for the steel S355. Residual stress relaxation is observed in all fatigue tests. Due to the High-Low sequence, residual stresses relax after the first interruption (M_1), when all amplitudes greater than 95% of the maximum amplitude $\sigma_{a,max}$ have been passed through. After the completion of the first block, residual stresses are almost stabilised at -50 to -100 MPa. Within the Low-High sequence, a sequential residual stress relaxation is observed after each load increment until the full spectrum length is passed through. After passing through the full spectrum length for the first time, the residual stresses remain almost stable or hardly change compared to the initial relaxation. Due to the higher maximum stress amplitudes within the linear spectrum compared

Fig. 9 Transverse residual stress profiles of HFMI-treated transverse stiffeners made of S700M after quasi-static tensile (left) and compressive loading (right)

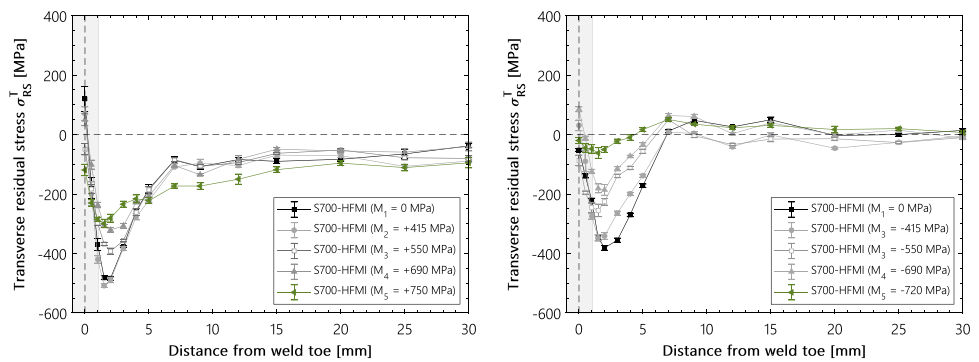


Fig. 10 Residual stress surface distributions during CAL, S355 (left) and S700M (right)

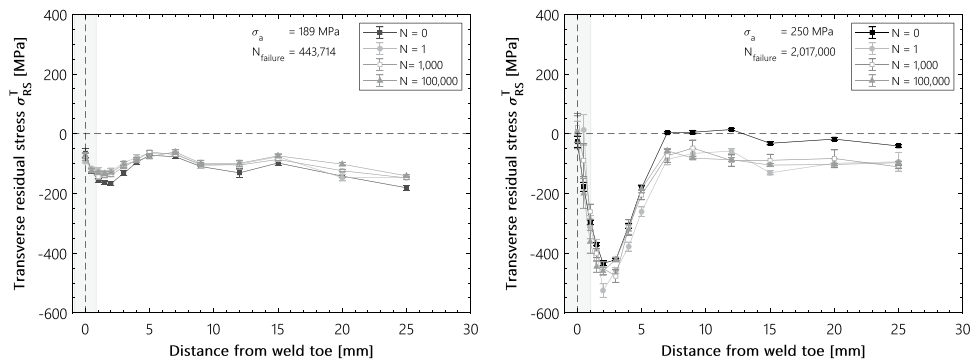
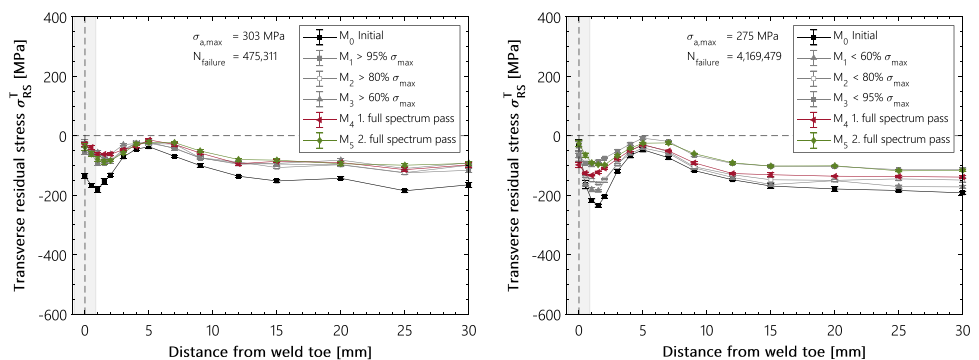


Fig. 11 Residual stress surface distributions of transverse stiffeners made of S355 during P(1/3) spectrum loading, High-Low (left) and Low-High (right)



to the P(1/3) spectrum, a higher residual stress reduction to zero or to even slight tensile stresses can be observed (Fig. 12).

Comparing the residual stress surface distributions of transverse stiffeners made of S700M in Figs. 13 and 14 with the measurements on HFMI-treated specimens made of S355, the following can be observed. Due to the low maximum stress amplitude within the P(1/3) relative to the material yield strength, no significant changes occur in the residual stress distribution due to the different load sequences. Whereas $\sigma_{a,max}$ of the linear shaped spectrum equals 80% of the S700M's yield strength. Thus, a change and reduction of the maximum residual compressive stresses occurs. Like the residual stress measurements on specimens made

of S355, there are no further relevant residual stress changes on HFMI-treated transverse stiffeners made of S700M steel after the first full spectrum pass.

Random loading The impact of random loading sequence of the P(1/3) and the linear shaped spectrum on the residual stress state of HFMI-treated TS of both materials is shown in Figs. 15 and 16. As described earlier, the residual stresses were measured at the end of a fully passed spectrum, after $N = 200,000$ cycles. After each measurement, the specimens were remounted in the testing rig and subjected to the same force signal as before. This procedure was repeated until failure of the specimen. In the case of the residual stress profiles displayed in Fig. 15 (P(1/3) spectrum), the last

Fig. 12 Residual stress surface distributions of transverse stiffeners made of S355 during linear shaped spectrum loading, High-Low (left) and Low-High (right)

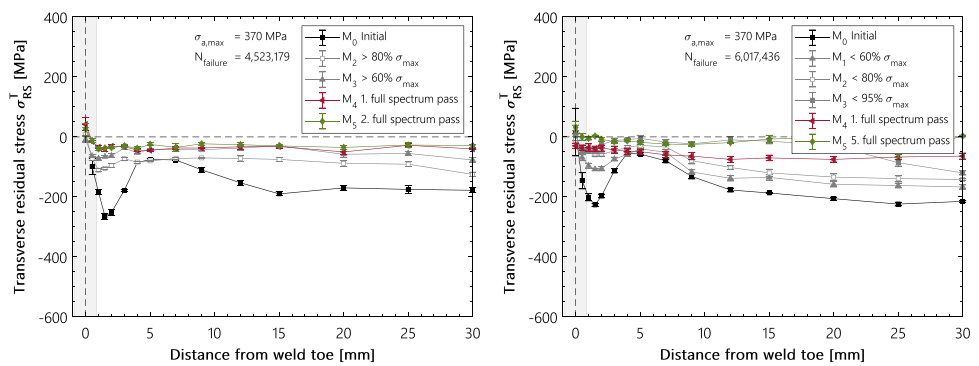


Fig. 13 Residual stress surface distributions of transverse stiffeners made of S700M during P(1/3) spectrum loading, High-Low (left) and Low-High (right)

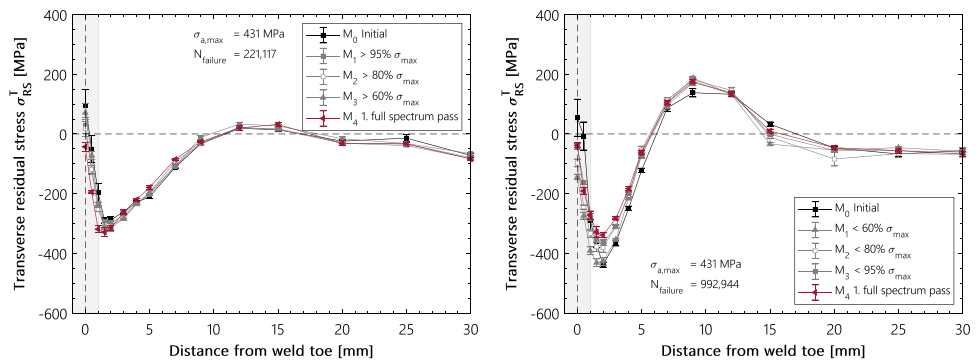


Fig. 14 Residual stress surface distributions of transverse stiffeners made of S700M during linear shaped spectrum loading, High-Low (left) and Low-High (right)

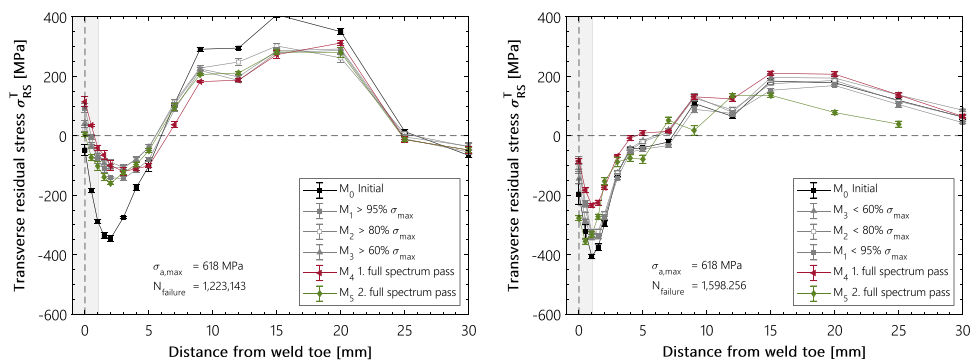


Fig. 15 Residual stress surface distributions of transverse stiffeners made of S355 after random VAL, P(1/3) spectrum (left) and linear shaped spectrum (right)

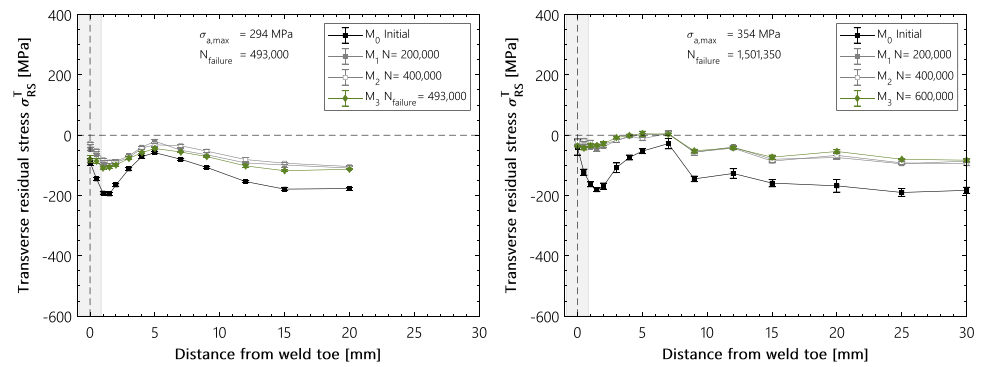
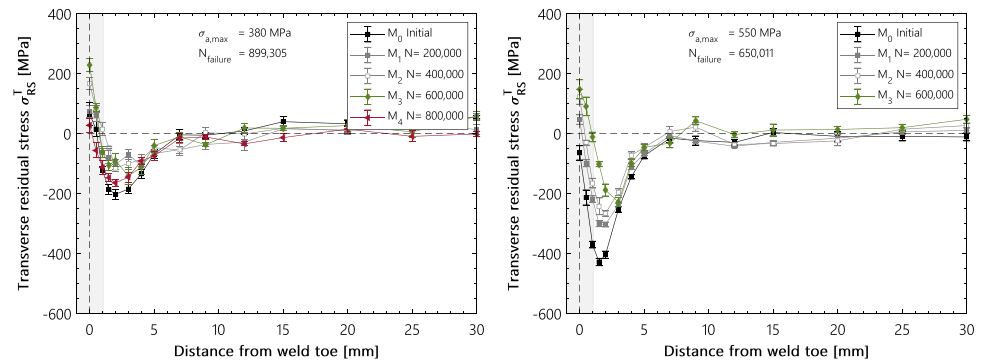


Fig. 16 Residual stress surface distributions of transverse stiffeners made of S700M after random VAL, P(1/3) spectrum (left) and linear shaped spectrum (right)



measurement could even be obtained after the test had terminated at 493,000 cycles, as the specimen did not fracture in the area of the measuring points.

As seen in the following figures, the effect of random loading sequence on the residual stress distribution remains comparable to the blocked High-Low and Low-High VAL. With the first full spectrum passed residual stress relaxation occurs in comparable height to the blocked spectrum. After the first full spectrum pass (M_1 , $N = 200,000$ cycles) residual stresses in loading direction seems to be almost stable. The higher maximum amplitudes of the linear shaped spectra compared to the P(1/3) has a significantly stronger impact on the residual stress relaxation.

4 Discussion

The evaluation of surface residual stress distribution of HFMI-treated transverse stiffeners subjected to different loading conditions shows the impact on the residual stress state. Both treatment devices produce uniform plastic deformations. At the weld toe, residual compressive stresses are present in loading direction, which adapt to the stress level of the base material with increasing distance from the weld toe. With increasing yield strength, higher residual stresses are obtained. For specimens made of S355, these residual

stresses vary between -150 and -250 MPa, for specimens made of S700M they range between -200 and -450 MPa. For both materials a characteristic half W-shape of the transverse residual stress appears. The maximum residual compressive stresses are found at the edge or next to the HFMI treated zone. The appearance and shape of the characteristic residual stress distributions may differ due to the treatment and preparation of the base material. The methods used, such as sandblasting and flame straightening, have a decisive impact on the stress distribution at the base material. Sandblasting was used to remove corrosion and other impurities from the surface of the base material. The HFMI treated zone as well as the area 5 mm in front of the weld toe were left out. The steel plates of the material S700M had to be flame straightened before the production and welding of the transverse stiffeners due to the high distortion. In some cases, tensile residual stresses of up to 400 MPa were induced. These residual tensile stresses are located between 10 to 15 mm from the weld toe. An influence of these tensile stresses on the fatigue behaviour has not been observed.

The investigations indicate that the induced compressive residual stresses remain almost constant under quasi-static loading up to a stress level of about 80% of the yield strength of the base material. When subjected to constant amplitude loading, specimens made of S355 and S700M show no significant residual stress relaxation. This is probably due to the low amplitude being applied. Even higher stress amplitudes

of 250 MPa (S355N) and 300 MPa (S700M), which correspond to 65 and 40% of the yield strength of the base material, cause only a slight change in the residual stresses, as described in [16]. The sequence effect on the residual stress stability for two different spectrum shapes is highlighted. The effect becomes visible within the first pass through the full spectrum length. While the residual stresses relax sequentially within the Low-High sequence with increasing stress level, the initial residual stresses are already reduced after all amplitudes greater than 95% of the maximum amplitude have been passed through when applying the High-Low sequence. Subsequently, no further residual stress relaxation is observed in further spectrum passes, and the loading sequence seems to have no further impact on the residual stress curve in the following.

During the fatigue test with random VAL, the residual stresses were recorded at the end of a fully passed spectrum. It is observed that after passing the spectrum for the first time, the compressive residual stresses are decreased. Analogous to the other loading sequences, no further significant relaxation occurs after further passes.

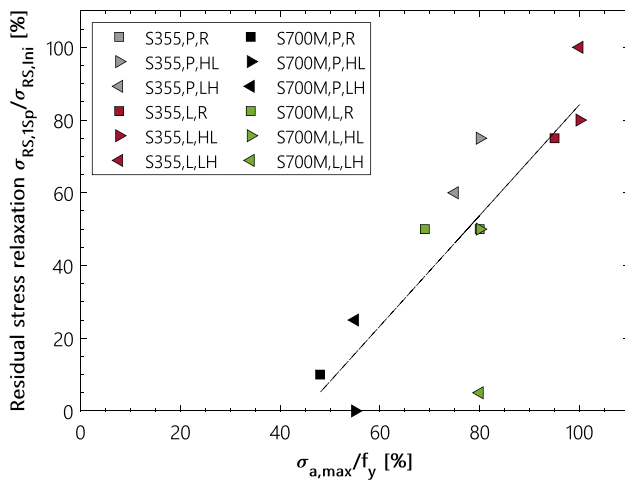


Fig. 17 Residual stress relaxation with respect to the applied maximum stress amplitude $\sigma_{a,max}$ relative to the yield strength f_y

Fig. 18 Failure locations (WT: Weld Toe, BM: Base Material) and Fatigue strength ($P_s = 50\%$) of TS in the AW and HFMI treated state [4, 5]



Figure 17 shows the ratio between the residual stress reduction after the first full spectrum pass and the initial maximum residual stress level in the HFMI-treated zone ($\sigma_{RS,sp}/\sigma_{RS,ini}$) versus the ratio between the maximum stress amplitude of the VAL and the yield strength of the base material ($\sigma_{a,max}/f_y$). A linear correlation between residual stress relaxation and the applied maximum stress amplitude in relation to the yield strength of the base material can be seen. In Fig. 17, tests with different loading sequences (R, HL, LH) with the P(1/3) and linear shaped spectrum are plotted, in which residual stress profiles were recorded. With an increase of the maximum amplitude in relation to the yield strength, there is a more pronounced decrease of compressive residual stresses. Significant relaxation of more than 50% of the initial residual stresses is observed under cyclic loading regardless of the sequence at a maximum stress amplitude of at least 70% of the material yield strength.

Figure 18 shows the fatigue strength values with a survival probability of $P_s = 50\%$ at $N = 2 \cdot 10^6$ load-cycles ($\Delta\sigma_{50\%}$) based on the statistical evaluation of the S-N data obtained by the VAL fatigue test in [4, 5]. The results of the experimental work confirm the fatigue improvement due to the HFMI treatment regardless of the level of residual stress relaxation. Both investigated steels showed a strong increase of the lifetime respectively the fatigue strength under all investigated spectra and load sequences. Figure 18 also provides a picture of typical fractures patterns of TS in the AW and HFMI-treated state. While in the AW state all specimens showed a typical fracture pattern in the weld toe, most specimens of the HFMI series failed in the base material. This indicates that the fatigue strength was locally increased by the HFMI treatment to such an extent that the strength of the base material becomes decisive for the fatigue performance of the component.

The comparison of the initial integral widths in Fig. 19 indicates a hardening of the S355 due to the HFH treatment. The line “Initial AW” represents the integral widths of the untreated samples, the line “ M_0 Initial” correspondingly those of the HFMI-treated weld toe. With the S700M, the difference between the two initial states is significantly greater compared to the S355. In fact, it is to be expected

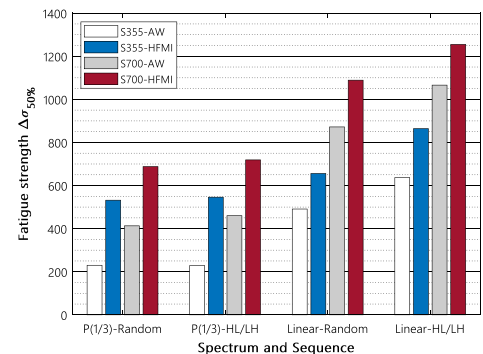
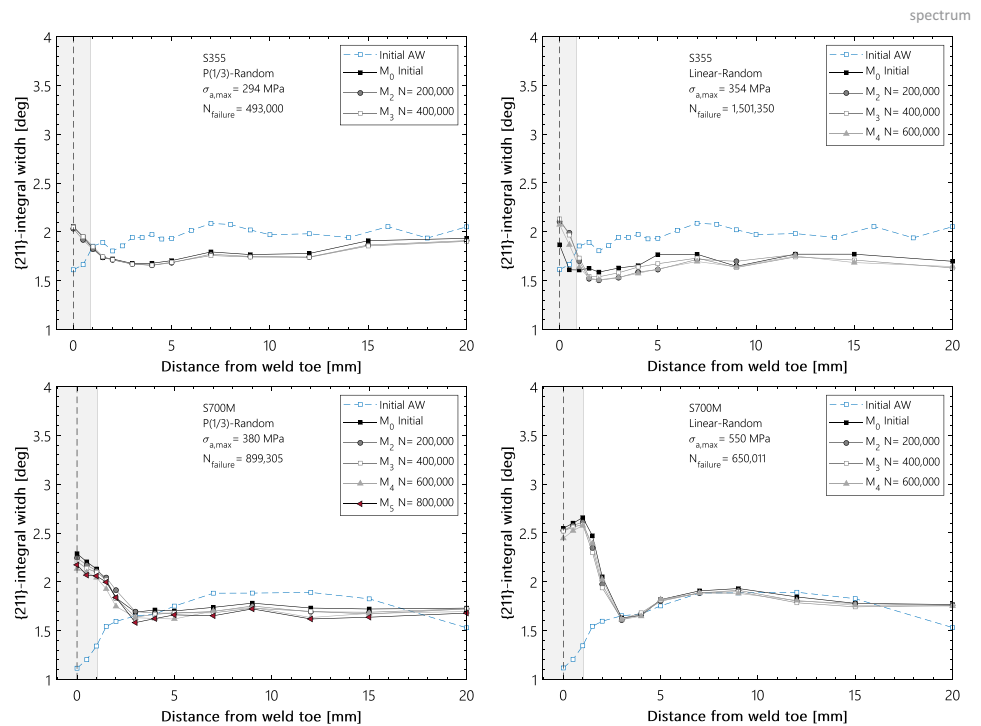


Fig. 19 $\{211\}$ -integral width distribution of transverse stiffener (S355, S700M) after random VAL, P(1/3) spectrum (left) and linear shaped spectrum (right)



that a more significant difference will appear for the material S355. The reason for the larger difference between the initial states in the AW-state and the HFMI-state of the material S700M could be a local softening caused by the welding process. Nevertheless, for both materials, the distribution of integral widths shows a local strain hardening induced by the HFMI treatment.

Furthermore, the distributions shown in Fig. 19 indicate that random VAL does not significantly affect the initial hardening condition of the treated surface layer. Slight differences between the curves with increasing number of load cycles can be attributed to the scattering of the measured values. Comparable results were received in VAL fatigue tests with HL and LH sequence [16].

Both investigated steels in the HFMI state show a strong increase of the fatigue strength under all investigated load conditions (Fig. 18). Concerning the observed significant residual stress relaxation, the increased fatigue strength of the S355-welds obviously is mainly related to the local notch improvement and strain hardening. The S700-welds appear to provide a reduced stress relaxation behaviour. Thus, the fatigue improvement can be related to compressive residual stresses, strain hardening and the improved weld toe geometry.

As mentioned above, studies [8, 9, 11] on longitudinal stiffeners show that the improvement factors by HFMI observed under VAL are much lower than under CAL. When the results of these studies are compared with those of this paper and those obtained by fatigue tests on transverse

attachments in [4, 5] it can be concluded that the potential of HFMI treatment for fatigue improvement under VAL must be evaluated in relation to the underlying local notch intensity of the component.

5 Conclusion

The aim of the presented study was to determine the effect of typical service loading on the fatigue performance of HFMI-treated transverse stiffeners made of different steel grades. In previous publications [4, 5], the evaluation of fatigue tests under VAL showed a strong increase in service life respectively fatigue strength under all load conditions applied. However, commonly, the strength-increasing and thus life-extending effect of HFMI treatment is mainly attributed to the induced residual compressive stresses. Therefore, in addition to the fatigue tests, the relaxation behaviour, i.e., residual stress stability under service loading, was monitored to evaluate the interaction between the improvement in fatigue strength and the modified local material condition. The results shown in this paper highlight that the residual stresses may be affected by VAL. The most significant effect on the relaxation of residual stresses is the magnitude of the maximum applied stress of the load spectrum.

However, the HFMI-treated specimens of both steel grades show a strong increase in fatigue strength regardless of the level of residual stress relaxation [4, 5]. It appears that the increased fatigue life due to the HFMI treatment must

be almost equally attributed to the hardened surface layer and the improved notch geometry. A special phenomenon observed during this study was the failure of the HFMI-treated specimens at the base material approx. 2–4 mm before the treated weld toe. This indicates that the fatigue strength was locally increased beyond that of the base material by plastic deformation of the weld toe.

Further experimental studies on different weld details and different steel grades as well as on varying mean stresses are recommended. It should be considered that the evaluation of the potential of the HFMI-treatment is not based solely on the residual stress stability. Relying solely on the induced residual stresses may lead to underestimation of the potential of these post weld treatment methods.

Acknowledgements The authors would like to thank the funding institution and the research association as well as the project committee for their support.

Conflict of interest The authors declare no competing interests.

Funding Open Access funding enabled and organized by Projekt DEAL. Open Access funding enabled and organized by Projekt DEAL. The IGF project 18.848 N of the Research Association on Welding and Allied Processes was funded by the German Federation of Industrial Research Associations (“Arbeitsgemeinschaft industrieller Forschungsvereinigungen,” AiF) within the framework of the programme for the promotion of Industrial Collective Research (“Industrielle Gemeinschaftsforschung,” IGF) of the Federal Ministry for Economic Affairs and Energy on the basis of a decision by the German Bundestag

Open Access This article is licensed under a Creative Commons Attribution 4.0 International License, which permits use, sharing, adaptation, distribution and reproduction in any medium or format, as long as you give appropriate credit to the original author(s) and the source, provide a link to the Creative Commons licence, and indicate if changes were made. The images or other third party material in this article are included in the article's Creative Commons licence, unless indicated otherwise in a credit line to the material. If material is not included in the article's Creative Commons licence and your intended use is not permitted by statutory regulation or exceeds the permitted use, you will need to obtain permission directly from the copyright holder. To view a copy of this licence, visit <http://creativecommons.org/licenses/by/4.0/>.

References

- Marquis GB, Barsoum Z (2016) IIW Recommendations for the HFMI treatment – for improving the fatigue strength of welded joints. Springer Singapore, Singapore, s.l.
- Stahlbau Verlags- und Service GmbH (2019) Ermüdungsbemessung bei Anwendung höhenfrequenter Hämmerverfahren. Stahlbau Verlags- und Service GmbH, Düsseldorf
- Schubnell J et al (2021) Residual stress relaxation in HFMI-treated fillet welds after single overload peaks. *Weld World* 65(11):2247. <https://doi.org/10.1007/s40194-021-01156-6>
- Schiller R et al (2021) Sequence effect of p(1/3) spectrum loading on service fatigue strength of as-welded and high-frequency mechanical impact (HFMI)-treated transverse stiffeners of mild steel. *Weld World*. <https://doi.org/10.1007/s40194-021-01121-3>
- Löschner D et al (2022) Sequence effect of as-welded and HFMI-treated transverse attachments under variable loading with linear spectrum. *Weld World*. <https://doi.org/10.1007/s40194-022-01302-8>
- Yildirim HC, Marquis GB (2013) A round robin study of high-frequency mechanical impact (HFMI)-treated welded joints subjected to variable amplitude loading. *Weld World* 32(11):1617
- Leitner M et al (2015) Fatigue strength of HFMI-treated high-strength steel joints under constant and variable amplitude block loading. *Procedia Eng* 101:251–258. <https://doi.org/10.1016/j.proeng.2015.02.036>
- Yıldırım HC, Marquis G, Sonsino CM (2016) Lightweight design with welded high-frequency mechanical impact (HFMI) treated high-strength steel joints from S700 under constant and variable amplitude loadings. *Int J Fatigue* 91:466–474. <https://doi.org/10.1016/j.ijfatigue.2015.11.009>
- Leitner M et al (2018) Fatigue strength of welded and high frequency mechanical impact (HFMI) post-treated steel joints under constant and variable amplitude loading. *Eng Struct* 163:215–223. <https://doi.org/10.1016/j.engstruct.2018.02.041>
- Leitner M et al (2020) Validation of the fatigue strength assessment of HFMI-treated steel joints under variable amplitude loading. *Weld World* 64(10):1681–1689
- Marquis G (2010) Failure modes and fatigue strength of improved HSS welds. *Eng Fract Mech* 77(11):2051–2062. <https://doi.org/10.1016/j.engfracmech.2010.03.034>
- Mikkola E, Remes H (2017) Allowable stresses in high-frequency mechanical impact (HFMI)-treated joints subjected to variable amplitude loading. *Weld World* 61(1):125–138. <https://doi.org/10.1007/s40194-016-0400-2>
- Leitner M, Khurshid M, Barsoum Z (2017) Stability of high frequency mechanical impact (HFMI) post-treatment induced residual stress states under cyclic loading of welded steel joints. *Eng Struct* 143:589–602. <https://doi.org/10.1016/j.engstruct.2017.04.046>
- Farajian-Sohi M, Nitschke-Pagel T, Dilger K (2010) Residual stress relaxation of quasi-statically and cyclically-loaded steel welds. *Weld World* 54(1-2):R49–R60. <https://doi.org/10.1007/BF03263484>
- Diekhoff, P. et al. (2022) Analysis of the residual stress stability of high frequency mechanical impact (HFMI)-treated transverse stiffeners of mild steel (S355) and high strength steels (S700) under p (1/3) and straight-line shaped spectrum loading.
- Löschner D et al (2020) Beanspruchungsreihenfolgeeinfluss auf die bearbeitungsbedingten Verfestigungen und Eigenspannungen und die Betriebsfestigkeit nachbehandelter Kerbdetails – Abschlussbericht zum Vorhaben IGF-Nr. 18.848 N. DVS Media GmbH, Düsseldorf
- Ummenhofer T, Weich I (2006) REFRESH – Lebensdauererlangung bestehender und neuer geschweißter Stahlkonstruktionen. *Stahlbau* 75(7):605–607
- Weich I (2009) Ermüdungsverhalten mechanisch nachbehandelter Schweißverbindungen in Abhängigkeit des Randschichtzustands. TU Braunschweig, Braunschweig Dissertation

Publisher's note Springer Nature remains neutral with regard to jurisdictional claims in published maps and institutional affiliations.